Vol. 41, No. 4 (2019) 498-515, DOI: 10.24874/ti.2019.41.04.04

Tribology in Industry

www.tribology.rs

RESEARCH

Effect of Load, Sintering Temperature and Reinforcement Concentration on Al-Si/γ-Al_2O_3/GNP Self-Lubricating Hybrid Composite

P.D. Srivyas[a,*], M.S. Charoo[a]

[a] *Mechanical Engineering Department, National Institute of Technology, Srinagar, Jammu and Kashmir, India.*

Keywords:

Friction
Wear
Self-Lubrication
Asperities
Automotive Applications

* Corresponding author:

Pranav Dev Srivyas
E-mail: devpranav.srivyas_17@nitsri.net

Received: 8 September 2019
Revised: 11 October 2019
Accepted: 25 October 2019

A B S T R A C T

Latest advancements in nanotechnology has lately empowered improvement of Hybrid nanocomposites for basic structural applications. Carbon based materials, graphite, carbon nanotubes (CNT's), and graphene have novel mechanical, tribological and thermal properties. Owing to their lubricious nature, drew scientists to integrate lightweight self-lubricating hybrid nanocomposites with prevalent mechanical and tribological properties for various automotive, aerospace and marine applications. Hence the objective of this investigation is to determine, the frictional and wear attributes of self-lubricating novel hybrid nanocomposites. Friction and wear studies of self lubricating Eutectic Aluminium Silicon/Nano Aluminium Oxide/Graphene Nano Platelets hybrid composite with varying GNP content. In the present examination, aluminum hybrid nanocomposites were fabricated by Spark Plasma Sintering (SPS) to consolidate γ-Al_2O_3 and Graphene nano-platelets (GNP) particles into Eutectic Al-Si to reinforcenanocomposites. For this novel composition sample; the impacts of load, the impact of fortification, impact of sintering temperature has been evaluated. The samples were set up at three sintering temperature 450 ˚C; 500 ˚C; 520 ˚C. To research the tribological conduct of self-lubricating hybrid nanocomposites, ball-on-disc tests were performed. The wear and friction behavior of the composites were assessed for loads (50, 100, 150, 200, 250, 300 N) with sliding distance of 120 meter; stroke2mm and frequency at 30Hz. Results of the tribo test indicate that the novel hybrid self lubricating composite exit excellent anti friction anf anti wear properties compared to Al-Si/nano Aluminium Oxide composite. Reduction in friction and wear of the hybrid composite was reported in the range 12.41–40 % and 87.76–92.97 % compared to Al-Si/Nano Aluminium Oxide composite sample. The outcomes demonstrated that sintering temperature, reinforcement concentration and operational parameters have huge impact on the properties of composite. It was discovered that this novel self-lubricating hybrid nanocomposites indicated predominant tribological properties and exhibited the capacity of self-lubricating composite amid tribological conditions. Frictional surfaces were explored utilizing

portrayal instruments such as Scanning Electron Microscopy (SEM), Electron Dispersion Microscopy (EDS), X-Ray Dispersive Microscopy (XRD) and 3-D Surface Profilometer.

1. INTRODUCTION

Wear in material is known to be one of the significant parameters to control their performances in long term. Wear is commonly depicted as the expulsion of material from the surface in relative movement by mechanical and nonchemical process [1-2]. Amid relative movement of two surfaces, different kinds of wear mechanisms, including adhesion wear, abrasion wear, delimitation wear, erosive wear, fatigue wear, and destructive/oxidative wear have been significantly reported [3-5]. The nature of wear can be comprehended by considering the surfaces of materials. Hybrid nanocomposites have demonstrated valuable effectiveness for various structural applications since they display critical increment in sturdiness, explicit quality, wear and annexation opposition, and can bear high temperature, when contrasted with the alloys [6]. Hybrid nanocomposites are surfacing as better substitutes for the regular aluminum composites. Specifically, tribological properties of hybrid nanocomposites have attracted much attention due to their applications as brake disc, cylinder liners and barrel of motor in vehicles. For a large portion of the hybrid nanocomposites, incorporation of ceramic particles can strikingly diminish the wear rate, by bearing the load capacity of the composite [7]. A sensible measure of information exists in the literatures on the sliding wear conduct of aluminum alloys& particulate-fortified composites.Considerable data is available on the consolidation of the hard-ceramic fortifications and soft solid lubricants into aluminum for improved wear obstruction. It is generally announced that the hard fortifications, improves the hardness and wear obstruction of the composites by improving the load bearing capacity. Gradually, they increment the wear rates of the counter faces leading to high coefficients friction at the contact [8-9]. Also, these hard particles withdrawn from the matrix, ensnared between the sliding surfaces and produced as third body abrasives; advanced worn surface damages [10].

Ongoing examinations demonstrate that the tribological properties of surface composites canbe additionally improved by including solid lubricant-particles or by hybrid self-lubricating composite [11]. This is because of increment in bulk mechanical properties, because of expansion of hard particles and reduction in contact coefficient friction because of development of lubrication film. Ongoing examinations have demonstrated that graphene as support in the framework / matrix can go about as a self-lubricating material prompting improvement in the tribological conduct of the hybrid composite [12]. Regardless, there are limited examinations about aluminum/graphene hybrid nanocomposites to reason about the impact of various materials and test parameters, i.e. effect of load, and weight % of graphene,nano-platelets on tribological conduct of the hybrid nanocomposites, etc.

Aluminum alloys have low yield stress and distorts broadly amid sliding contact while graphene particles in composites improves the twisting and discontinuity of the surface and sub-surface by giving a persistent film of graphene on the contact surfaces after short run-in period. The graphene lubrication film obstructs direct metal to metal contact and henceforth forestalls seizure [13]. Dispersion of fortifying particles in a surface layer is hard to accomplish utilizing traditional surface adjustment (fabrication) methods dependent on high temperatures. In this specific research Spark Plasma Sintering (SPS) [14-15] non-conventional fabrication route is utilized. Sintering is the way toward making objects from powder, by warming the material in a heater lowerthan its melting point with the goal that holding takes place by dispersion of particles. Spark Plasma Sintering fabrication takes just a couple of minutes to finish sintering procedure contrasted with regular sintering which may take hours or even days for the equivalent. This

high sintering rate is conceivable in SPS. Likewise, sintering time is decreased because of less holding time, often 5 to 10 minutes. Synchronous use of temperature and load prompts a high densification and consequently an increase sintering temperatures from 200 to 250°C indicates sintering is therefore, effectively acquired.In SPS, since no coarsening and grain development was permitted to happen, high relative densities were achieved in extremely brief time. Nano estimated powders can be sintered without impressive grain development which is not possible in regular sintering process.In SPS the powder is continuously poured into the graphite and the die is encased with reasonable blows. This whole setup together is legitimately put into the SPS chamber and spacers are utilized if important. The chamber is then shut and the environment (vacuum, Argon and so on) in which sintering is to be completed is connected in the chamber. The program is set into the control unit and sintering is completed. Because of preferred standpoint of high warming rate and less holding time, SPS can limit the undesirable sintering responses in profoundly receptive frameworks thus, development of unwanted item stages can be avoided.

Studies about detailed analysis in this field are summarized below: Liu et al. [16] reported a direct connection between the wear volume and load for laser prepared Al– Gr composites with 1.55 wt.% Gr. It was reported that the wear has been fundamentally affected by the arrangement of a lubricating film of Gr particulates and expulsion of worn material was seen subsequent to the disappointment of this film. Lin et al. [17] have researched Al/Gr composites with 0– 6 wt.% Gr and the outcomes demonstrate diminished wear rate with increment in particulate substance. Lessening of wear has been credited to counter-action of direct contact of sliding surfaces and decreased furrowing impact of Al chips because of the speedy arrangement of lubricating film of graphite particulates. Krisnamurthy et al. [18] in their examination on machining of Al–Gr composites has demonstrated extensive decrease of cutting powers and this has been ascribed to the conceivable decrease of rubbing because of strong grease of Gr particulates. Das et al. [19] have talked about on development of Mechanical mixed layer (MML) comprising of debris and fragments of SiC particles. SiC in MML and in the subsurface locale are divided into better particles in this manner, exhibiting the event of subsurface amid grating wear of LM13– SiC composites. Ted Guo and Tsao [20] reported that expansion of Gr particulates encourages simple machining and results in diminished wear of Al– Gr composites contrasted with Al alloy. In any case, high measure of Gr may result in increment of wear because of reduction in break strength with increment in % support of Gr particulates. Ted Guo et al. [21] have seen that wear of Al– 10SiC– 2– 8Gr increments up to 5%Gr in view of diminished break durability and afterward diminishes because of development of thick strong lubricating film which abrogates the impact of crack sturdiness durability. Hassan et al. [22] have detailed a decline in hardness with increment in % support of Gr because of expanded porosity. Riahi et al. [23] studied the impact of tribo-layer containing basically Gr on wear of Al–10SiC–4Gr composites. Basavarajappa et al. [24] in theirexaminations on Al–15SiC–3Gr composites have demonstrated that the level of subsurface twisting and in this way the wear rate in graphite composites is not as much as that of graphite free composites. Rohatgi et al. [25] announced that decrease in friction coefficient (COF) of Al–10SiC–6Gr is because of the mix of increment in mechanical properties because of expansion of SiC and development of graphite film. Ghazaly et al. [26] have orchestrated the aluminum/graphene composites at various weight % (0.5, 3 and 5 wt.%) by utilizing powder metallurgy strategy. A blend of cold compaction and hot expulsion at ~0.45 Tm (305 °C) were utilized to integrate aluminum/graphene self-lubricating nano composites. In their examination, the impact of weight level of graphene on wear rate of self-lubricating nano composites was explored. The outcomes demonstrated that self-lubricating composite fortified by 3 wt.% graphene has the best tribological properties under dry wear test conditions when contrasted with unreinforced and different arrangements of graphene strengthened composites. The outcomes demonstrated that the scratches, pits, delamination of AA2124/3wt.% graphene composite were essentially not as much as that of unreinforced AA2124. Unreinforced compound displayed serious wear routine and AA2124/3wt.% graphene composite showed gentle wear routine. Generous work has been

completed to contemplate different properties to create appropriate materials for extreme administration Conditions, where weight decrease in relationship with low coefficient of thermal extension, higher heat conductivity, better temperature capacity and great wear obstruction are of prime contemplations. In the present examination, the impact of tribological parameters, materials factor and sintering parameter on wear and friction conduct of the hybrid composites are explored.

2. EXPERIMENTAL PROCEDURE

2.1 Raw Material and Powder Mixing

Al-Si eutectic powder (APS) 60-70 μm; γ-Al2O3 20 nm; GNP 2-6nm thickness utilized as the crude material for the composite. The GNP reinforcement is first sonicated in ethanol in a ultrasonic probe sonicator for 2 hours followed by 2 hours sonication after adding γ-Al_2O_3 and finally 2 hours more after adding matrix material. After this the suspension is then blended further in high vitality planetary ball milling machine to make homogeneous mix. For the handling framework, powder was stacked in a silicon nitride compartment. Wet mixing was done in ethanol medium which used as the Process Controller Agent (PCA) prevents weld of the powder with the mixing jar wall. Silicon nitride ball of diameter 10 mm estimation were used for the blending with weight extent of ball to powder is 10:1. Preparing was performed at 240 rpm for 12 hours with a regular break of 15 minutes for2 hours.After the preparing strategy, the materials were mixed in suspension of matrix containing in ethanol, which was dried in a vacuum evaporator at 50 °C temperature for 3 hours. Any water of crystallization was removed by warming the specimen in the vacuum oven at the expected temperature of 50 °C for an hour to absolutely expel the sogginess content. To maintain a strategic distance from oxidation of the powder, the prepared powder was kept in the glove box to restrain the spoilingsuch as oxidation of the produced powder.

2.2 Sample Fabrication and Prepration

Two creations were mixed; Al-Si–6wt.% γ-Al_2O_3–4wt.% GNP and Al-Si–6wt.% γ-Al_2O_3–5wt.% GNP. Handling of the powder with different wt.% parameters was made using Spark Plasma Sintering (SPS) [Dr. Sinter-SPS-625, FujiElectronicINDUSTRIALC0. Ltd. JAPAN] route. Take known amount of dried and processed test powder in a round and hollow die, fixed with graphite sheet which encourages simple evacuation of the sample after sintering. Switch on the Chiller – blower and the machine. Spotting the die containing the powder test inside the SPS chamber. At that point, set the optimal (time-temperature information) required for the examination to pursue and from that point, maintain the required environment (Vacuum, Argon and so forth) inside the chamber. Additionally, set the z-hub position to zero. Switch on the clock lastly, and activate sinter to begin the sintering procedure. For estimating the temperature in SPS two kinds of instruments are utilized: thermocouple for sintering temperatures lower than 1000 °C and pyrometer for sintering temperatures of around 1000 °C. High DC Pulse is passed between graphite anodes and pivotal weight at the same time, connected from the earliest starting point of the sintering cycle. After the sintering, the power is cut and the specimen is permitted to cool. By using SPS creation course most extraordinary temperature up to 2400 °C can be cultivated to produce test by using standard graphite die on of measurement 30mm for the making of the example in the SPS. The sintering process was done at 450 °C; 500 ˚C and 520 ˚C Sintering temperature for all the composite example at warming rate of 100 °C/min; consistent load of 50 MPa all through the whole methodology; holding time 10 minutes under argon air (Fig. 1). The sintering is done in controlled air which enables controlled abatement and prompts the formation of totally dense samples (Table 1) (Fig. 2). This system does not require any folio and pre-compaction as the compaction and sintering goes inseparably. Clear grain limits; increase in flexibility; improved interfacial holding; confinement of diminished corruptions are key achievements of this assembling course. The whole technique of making of test takes 14 minutes 30 seconds. For the composition Al-Si–6wt.% γ-Al_2O_3–4wt.% GNP at 520 ˚C the powder sample comes up short i.e the example liquefies and vanishes which causes failure of this composition at this temperature. The sintered examples were then expelled from the die after fast cooling technique. The sintered precedents were then cleaned by utilizing cleaning machine using SiC emery paper with grit

size varying from 220-2000 coarseness measure. The samples were then cleaned using diamond paste and aerosol spray (5-0.25 μm) on the velvet paper to get the mirror cleaned surface.

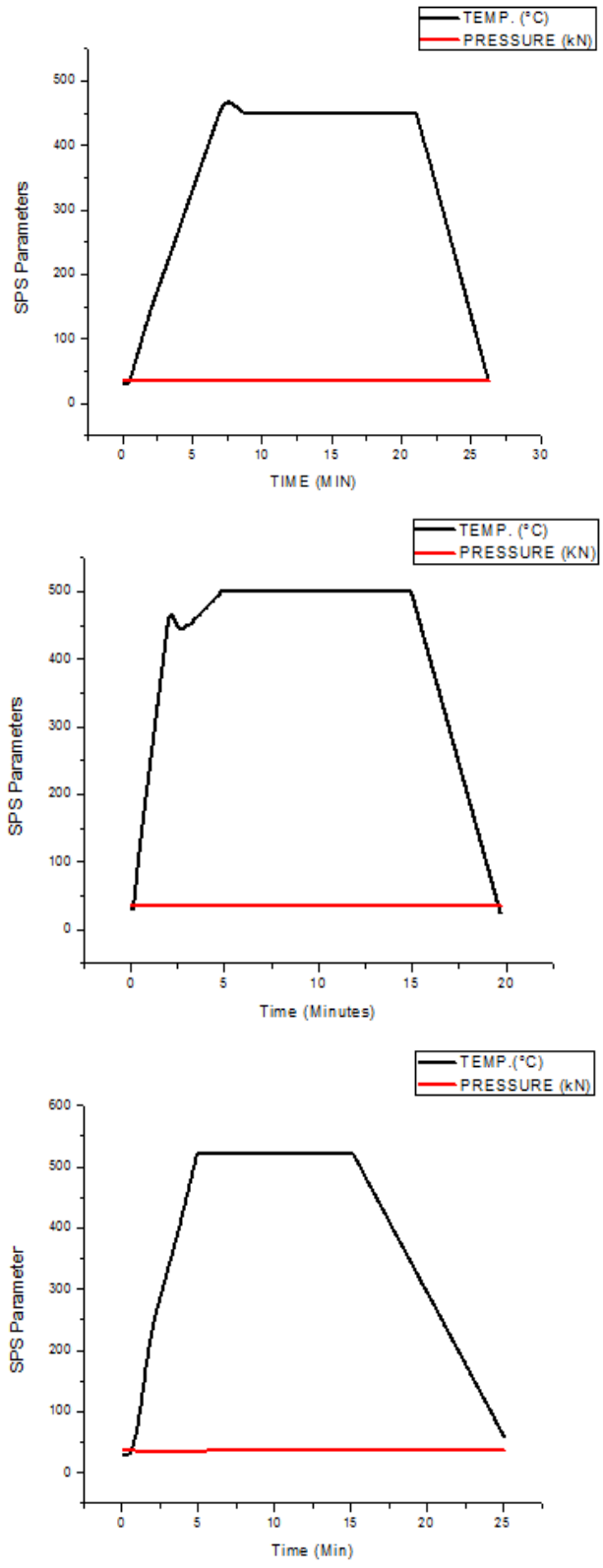

Fig. 1. SPS parameter variation with time. (a) sample fabricated at 450 ˚C; (b) sample fabricated at 500 ˚C; and (c) sample fabricated at 520 ˚C.

Table 1. Density and Porosity of the fabricated composite sample.

Composition & Sintering Temp.	Reinforce wt.%	Theoretical Density (g/cm³)	Practical Density (g/cm³)	Porosity Content (vol.%)
Hybrid Composition 5 (HC5-450) 450˚C	Al-Si +6 wt.% Al_2O_3 + 4 wt.% GNP	2.727	2.5229	7.4844
Hybrid Composition 5 (HC5-500) 500˚C	Al-Si +6 wt.% Al_2O_3 + 4 wt.% GNP	2.727	2.6698	2.0975
Hybrid Composition 6 (HC6-450) 450˚C	Al-Si +6 wt.% Al_2O_3 + 5 wt.% GNP	2.724	2.4972	8.32599
Hybrid Composition 6 (HC6-500) 500˚C	Al-Si +6 wt.% Al_2O_3 + 5 wt.% GNP	2.724	2.6631	2.2356
Hybrid Composition 6 (HC6-520) 520˚C	Al-Si +6 wt.% Al_2O_3 + 5 wt.% GNP	2.724	2.6913	1.200

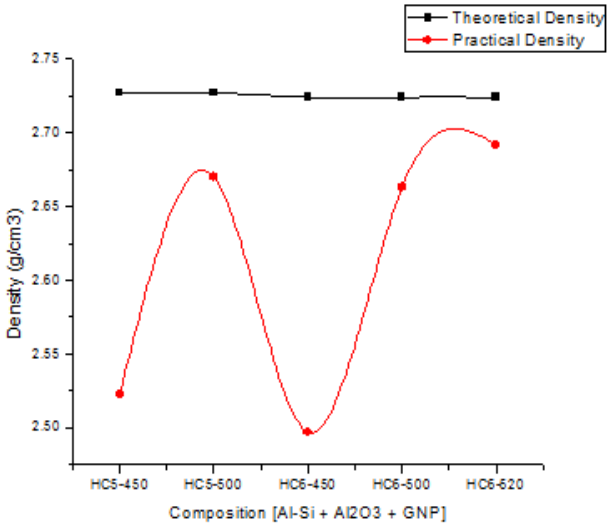

Fig. 2. Density graph with respect to reinforcement concentration & sintering temperature.

2.3 Testing and Characterization

Hardness studies were carried out on polished hybrid composites specimens using HVD-1000 MP Digital micro hardness tester. Hardness tests were performed thrice on the samples with different compositions, fabricated at different temperature to determine the hardness number of the Spark Plasma Sintered analysis. In Vickers hardness studies, at certain load and for certain dwell time composite samples were associated with diamond indenter, and after load removal it was analyzed using optical microscope. To determine the hardness number indentation load and area of residual impression ratio is

used. Dry sliding tribological test were also directed on Ball-on-Disk Reciprocating Tribometer (R-Tech Universal Tribometer) in at Room Temperature. The tribometer is sensor controlled and has appropriate information acquisition framework which is utilized to execute test and to spare the yield results. The tribo tests were ran for the differing load (50-300 N); with different parameter stroke 2mm; recurrence 30 Hz; Sliding Distance 120 meter at consistent rate. For tribological test the counter-body utilized is the chrome steel ball plated with chromium. Each test samples were appropriately cleaned with the acetone in the ultrasonic shower,in order to expel the polluting influences from the example surface and after that drying in the vacuum oven. Different instruments for example SEM (HITACHI S3600N), EDS (HITACHI S3600N), 3-D Surface Profilometer (R-tech USA) and Optical Microscopy (Leica DM 6000M) were utilized for the different pre just as post testing portrayal. Fig. 3. Shows the processing flow scheme of the experimental procedure.

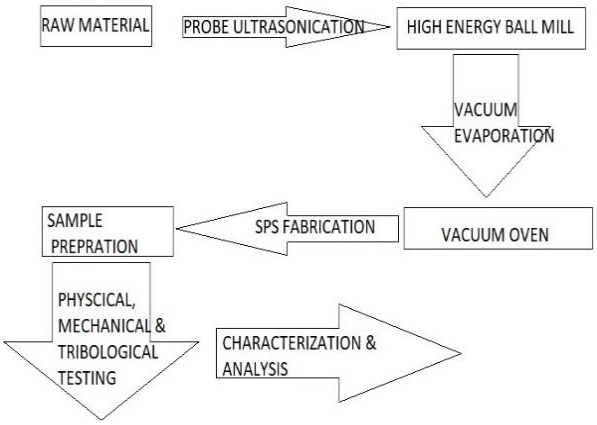

Fig. 3. Processing Flow scheme of the experimental procedure.

3. Friction and Wear Studies

Ball-on-disc reciprocating tribological tests were conducted at Room temperature under dry conditions to study friction and wear of tribo-pair. Load test (50N-300 N) was performed in this study with other parameters i.e. sliding distance (120 m), frequency (30 Hz),stroke (2 mm),in a constant state. In addition, scar wear volume was calculated using 3D-Profilometer. Moreover, to determine the wear rate equation 1 was used.

$$Wr = \frac{Wv}{SD \times L} \quad (1)$$

Wr: Wear Rate;
Wv: Wear Volume;
SD: Sliding Distance;
L: Load

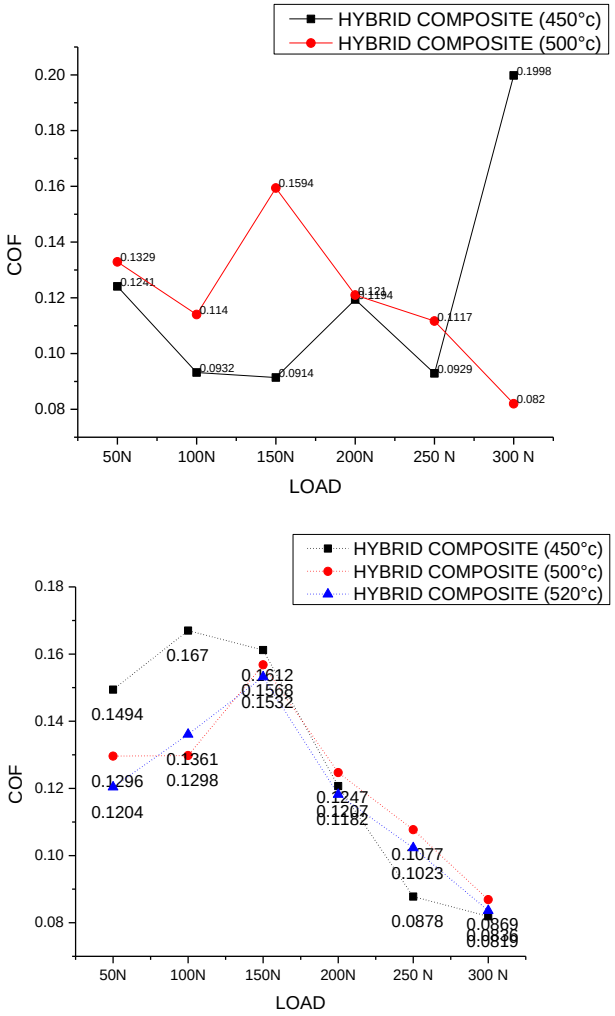

Fig. 4. Load v/s COF graph for different composite samples fabricated at variable temperatures. (a) Hybrid Composition 5 [Al-Si+6wt.% Al_2O_3+4wt.% GNP]; (b) Hybrid Composition 6 [Al-Si+6wt.% Al_2O_3+5wt.% GNP].

Figure 4 shows COF verses load results for different compositions specimens. Wear volume verses load graph is shown in the Fig. 5. Wear Coefficient verses load graph is shown in Fig. 6. COF for HC5-450 is shown in Fig. 4a. For HC5-450 COF first decreases as load increases from 50-150 N load and achieves the lowest value of COF (0.0914) and then increases to 200 N load and then further rises unto 250 N load. Maximum value for the COF was obtained at 300 N load (0.1998). Form Fig. 4a, HC5-500 sample i.e. 4wt.% GNP composite sample fabricated at 500 ˚C shows maximum COF value at 150 N load

(0.1594) and minimum at 300 N load (0.082). Continuous decrease in the COF was reported for this composition after 150 N load. Maximum (0.167) and minimum (0.0819) COF was observed at load 100 N and 300 N load respectively for HC6-450 sample. COF continuously decreases for HC6-450 from 100-300 N load, as shown in Fig. 4b. In HC6-500, COF trendfirst continuously increased up to 150 N load (0.1568) and further decreased with load and achieved minimum COF at 300 N (0.0869) shown in Fig. 4b. For HC6 - 520, shows similar trend as HC6-500, with the increase in the COF value up to 150 N load (0.0836) and then further decrease and achieve minimum COF (0.0836) at 300 N load, shown in Fig. 4b.

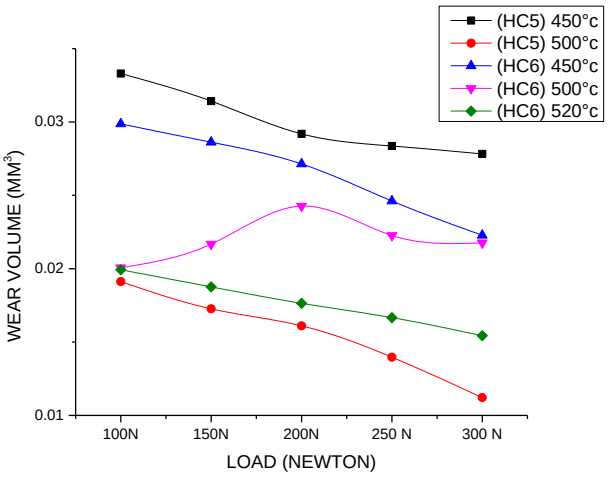

Fig. 5. Load v/s wear volume graph for samples fabricated at variable temperatures.

Wear volume for HC5-450, decreases with load. Maximum (0.033299 mm³) and Minimum (0.0278256 mm³) wear volume was reported at 100 N and 300 N load respectively. HC5-500 shows similar trend as HC5-450, but comparatively less wear volume was reported. Minimum wear volume (0.0112161 mm³) at 300 N and maximum (0.019123 mm³) at 100 N load was reported. The wear volume for HC6-450 decrease as load increases. Wear volume, minimum value (0.022276 mm³) and maximum (0.029869 mm³) was reported at 300 and 100 N load respectively. HC6-500 shows minimum wear volume of (0.0200654 mm³) at 300 N and maximum wear volume (0.0242655 mm³) at 200 N load. HC6-520 reported maximum (0.019929 mm³) and minimum (0.015433 mm³) wear volume at 100 and 300 N load. Wear coefficient for HC5-450 gradually decrease with load (Fig. 5).

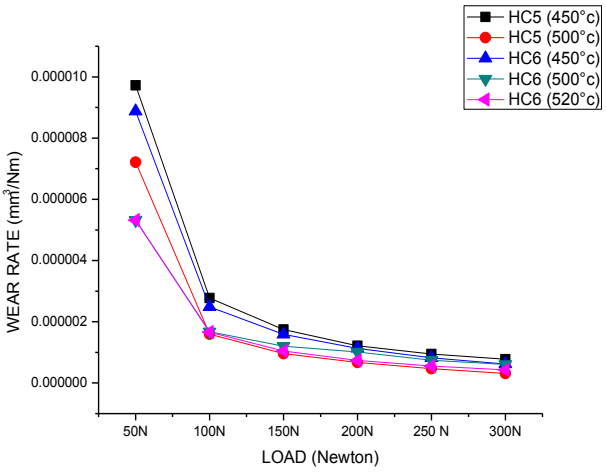

Fig. 6. Load v/s wear rate graph for samples fabricated at variable temperatures.

Wear coefficient maximum (9.72103E-06 mm³/Nm) and minimum (7.72934E-07 mm³/Nm) was obtainedat load 50 and 300 N respectively. Wear coefficient for HC5-500 shows decreasing trend with increasing load. Maximum wear coefficient (7.2109E-06 mm³/Nm) for 50 N and minimum (3.11558E-07 mm³/Nm) for 300 N was obtained. Wear coefficient for HC6-450 (8.87372E-06 mm³/Nm) maximum and (6.18776E-07 mm³/Nm) minimum was reported at 50 N and 300 N load. Maximum wear coefficient (5.31603E-06 mm³/Nm) at 50 N and minimum of (6.04563E-07 mm³/Nm) at 300 N load was reported for HC6-500. Wear coefficient for HC6-520 minimum (4.28685E-07 mm³/Nm) at 300 N and maximum (5.31603E-06 mm³/Nm) at 50 N load was observed (Fig. 6).

4. Hardness

The effect of indentation load (100, 300 and 500 gf); dwell time (10, 12 and 15 sec); reinforcement concentration and sintering temperature on hardness properties of all the fabricated specimens were studied (Fig. 7) (Table 2). GNP reinforcement has an impact on the hardness properties of the composite samples. It was observed that with an increase in the secondary reinforcement reduction in the hardness value of the composite was reported. This reduction was due to the introduction of soft reinforcement particles, which a huge impact on the hardness properties. Impact of sintering temperature is also very crucial for achieving good hardness properties of the composite specimens.

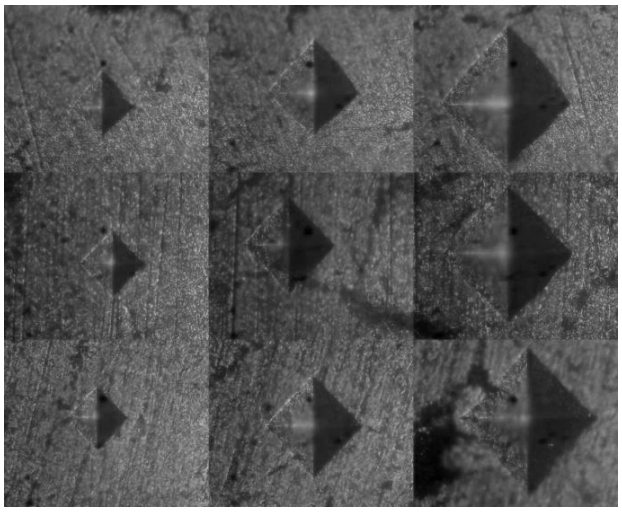

Fig. 7. Micro Indentation of Vickers Hardness test.

Table 2. Hardness Value (Vickers Hardness Test) for hybrid composite samples.

Hardness Value [Hybrid Composite 5 – 450]				
Sintering Temperature 450 °C				
Dwell Time↓	Load →	100 gf	300 gf	500 gf
10 sec		60	76	69
12 sec		57	73	65
15 sec		53	70	62
Hardness Value [Hybrid Composite 5 – 500]				
Sintering Temperature 500 °C				
Dwell Time↓	Load →	100 gf	300 gf	500 gf
10 sec		68	87	79
12 sec		64	81	75
15 sec		63	77	73
Hardness Value [Hybrid Composite 6 – 450]				
Sintering Temperature 450 °C				
Dwell Time↓	Load →	100 gf	300 gf	500 gf
10 sec		59	73	65
12 sec		55	76	63
15 sec		52	67	66
Hardness Value [Hybrid Composite 6 – 500]				
Sintering Temperature 500 °C				
Dwell Time↓	Load →	100 gf	300 gf	500 gf
10 sec		66	85	77
12 sec		63	80	73
15 sec		61	76	71
Hardness Value [Hybrid Composite 6 – 500]				
Sintering Temperature 500 °C				
Dwell Time↓	Load →	100 gf	300 gf	500 gf
10 sec		84	100	85
12 sec		81	90	82
15 sec		80	87	77

Composite sample with reinforcement 5 wt.% GNP fabricated at 520 ˚C shows maximum hardness value which ensures the significance of sintering temperature on hardness property. Indentation load is another crucial factor that affects the hardness properties of the composite. From the results, it was reported that microhardness significantly depends on reinforcement concentration, sintering temperature as well as the applied indentation load. Effectuality of dwell time was not so significant for hardness value of hybrid composite samples.

5. WEAR CHARACTERIZATION

Two main factors that affect to generate friction and cause wear of the material are: adhesion and ploughing asproposed by Bowden and Tabor [27]. Another wear mechanism namely Plastic deformation/diffusion has been additionally identified. The factor includes: adhesion of material on the sliding surface region; ploughing by hard asperities as well as wear debris (third body abrasion); relative parameters i.e. sliding speed, tribo-environment and counter body. But in general; ploughing and asperities deformation effect is greater than adhesion.

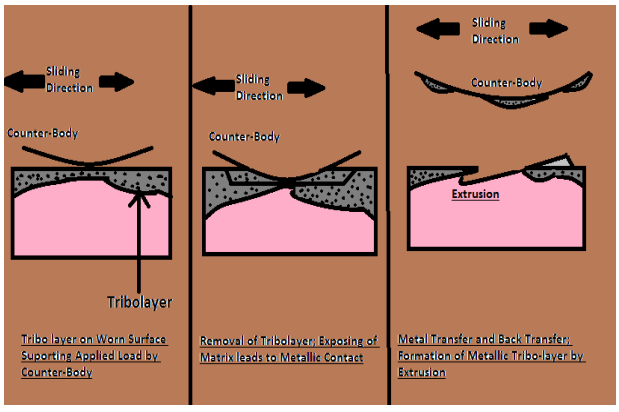

(a)

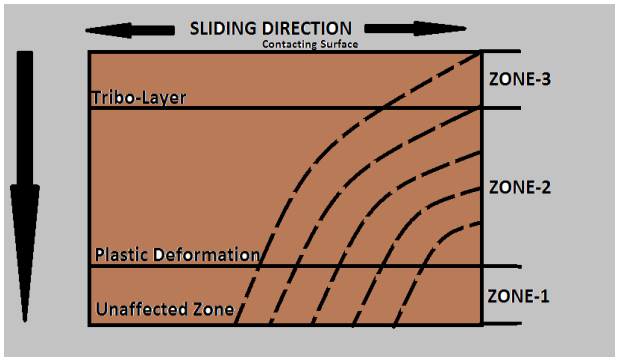

(b)

Fig. 8. (a) Tribo layer; removal of tribo layer and metal transfer mechanism; (b) Wear Zone catogrization.

Transition in wear mechanism from mild to severe wear is because of the formation of metal debris as the result of wear which further induces third body abrasion. These deformities produce surface reaction films caused by oxidation and reduction within the tribo-testing environment. These surface reaction films control the wear at low load but as the load increases the transition of mild wear to severe wear take place. In case of aluminum the wear of metal is improved by adding silicon,which improves the oxide layer surface support and reduces metal to metal contact while testing. Al-Si alloy mainly exhibits two type of wear mechanisms i.e. (a) below transition load, in which, oxides are produced and (b) at critical load; dependency on the tribo condition and body counts, which produces metallic wear, metal particle transfer and production of metal debris (Fig. 8).

Optical micrographs of dry sliding wear scar were observed for the analysis of the wear mechanism (Fig. 9). It was noticed that a high wear was observed if there was direct asperity-asperity contact which leads to prone abrasion. Mutual transfer of the material was observed using optical micrographs. For dry wear scar, severe plastic and shear deformation, crack, metallic wear as well as scuffing and seizure were the main wear mechanism. The presence of the graphene oxide tribo-layer provides lubrication to the tribo-pair. Protective lubrication film prevents direct contacts and reduces the wear and COF. Dense grooves in the optical micrographs give the evidence of dominated abrasive wear. For higher sliding distance and at high load strong tribo-layer/oxide layer formed, prevents direct metal contact. Metallic and seizure wear was predominant at 300 N applied load. Seizure was the probable wear mechanism at this wear regime. Very high applied load was characterized by formation of interfacial molten film between interfaces. Howell and Ball [28] characterized molten film formation as melt wear in the composite. It was reported that molten layer of metal matrix compositetrapped between the nonmelted metal matrix composite and counter body. This wear mechanism report minimized wear and low COF.

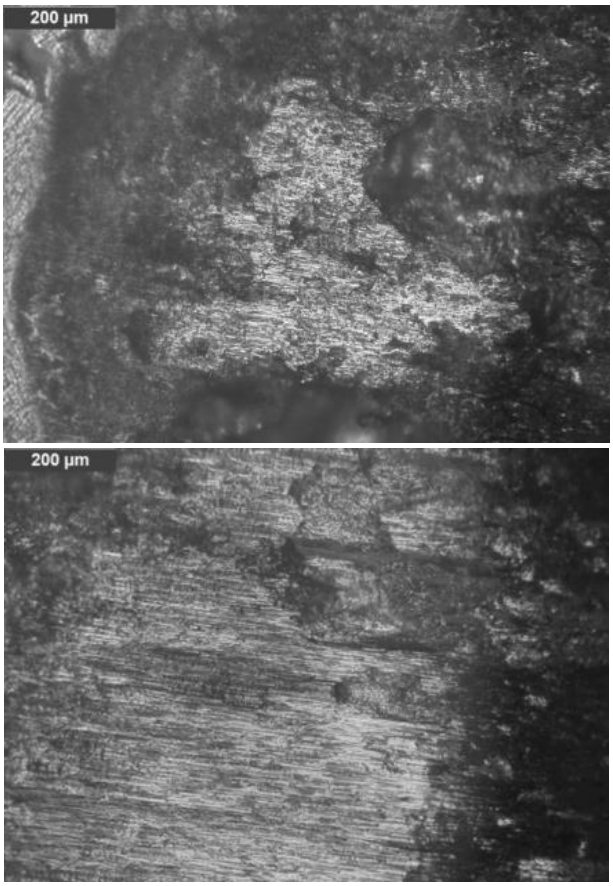

(a) Hybrid Composition 5 (450 ˚C) [50 N; 300 N]

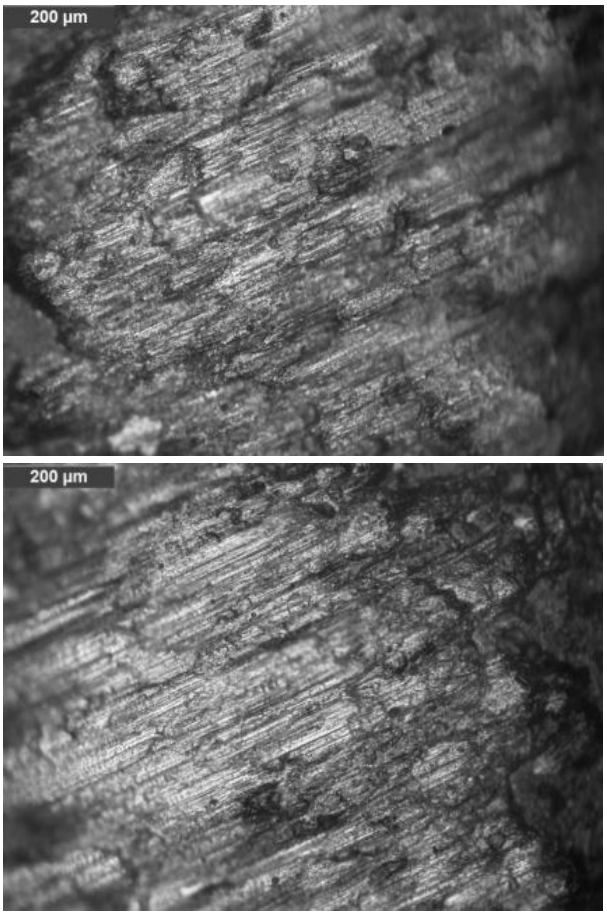

(b) Hybrid Composition 5 (500 ˚C) [50 N; 300 N]

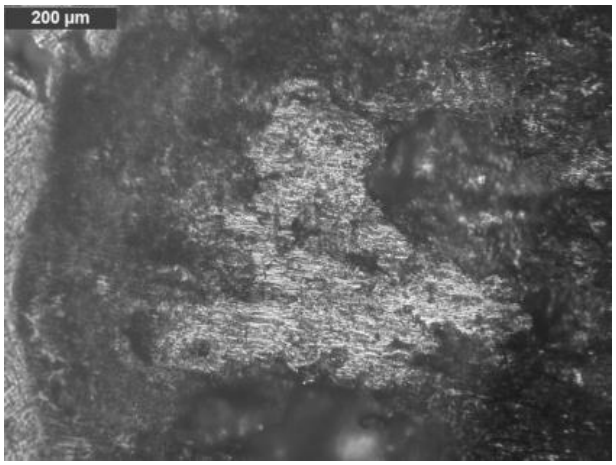

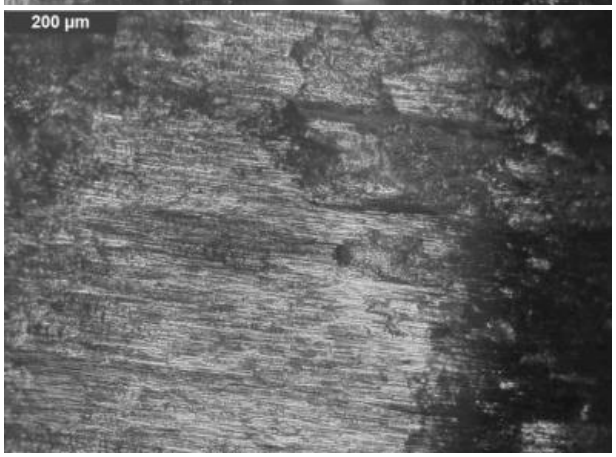

(c) Hybrid Composition 6 (450 ˚C) [50 N; 300 N]

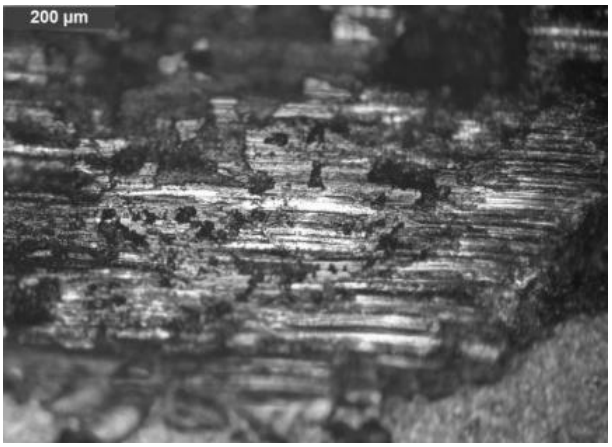

(d) Hybrid Composition 6 (500 ˚C) [50 N; 300 N]

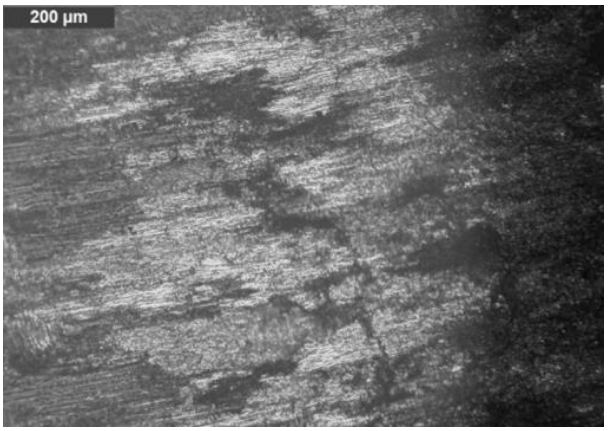

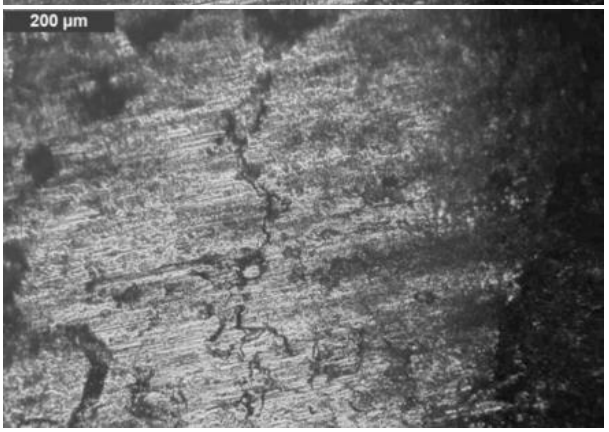

(e) Hybrid Composition 6 (520 ˚C) [50 N; 300 N]

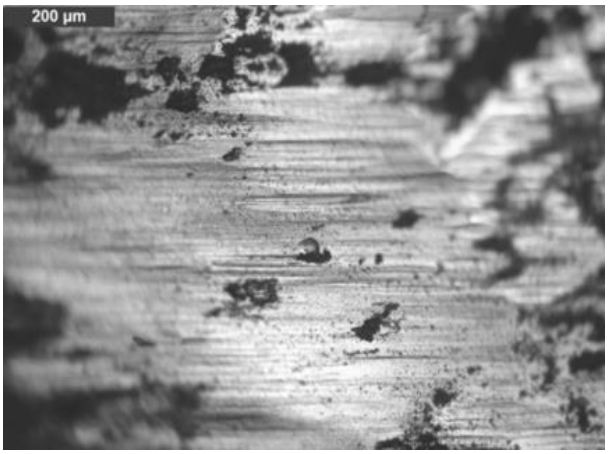

(f) Optical counter body

Fig. 9. Optical Micrographs of the wear scar on hybrid composite sample and counter body.

Wear mechanism analysis was conducted by using SEM micrographs (Fig. 10). It was reported that in all the cases the dominant wear mechanism was delaminating wear as well as abrasion in mild wear regime and adhesion; scuffing, seizure and melt at severe conditions for high applied load. From SEM analysis it was clear that graphene tribo-layer formed homogeneously adheres to the scar surface and act as the protective layer to prevent direct metallic contact between the counter body and hybrid composite surface. The two-dimensional sheet of graphene prevents easy shear due to wear Vander-wall force and this shearing under the sliding surface reduced shear stress and plastic deformation in the sub-surface region. Protective layer acts as the solid lubrication film and provides self-lubrication properties. EDS analysis was done and it was revealed that carbon and oxygen are present which conforms the formation of graphene oxide layers (Fig. 11). Raman analysis gives evidence to the EDS studies. At severe loading conditions, seizure and melt wear observed by SEM images. A melted layer was observed on the wear surface.Outputs of SEM and EDS analysis are shown in Figs. 10 and 11.

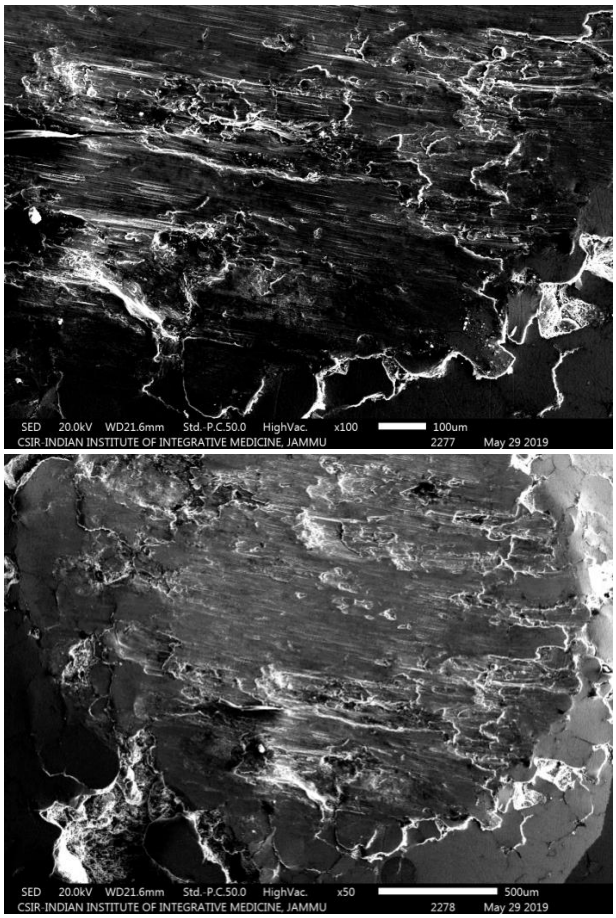

(a) Hybrid Composition 5 (450 ˚C) [50 N; 300 N; x50, x100]

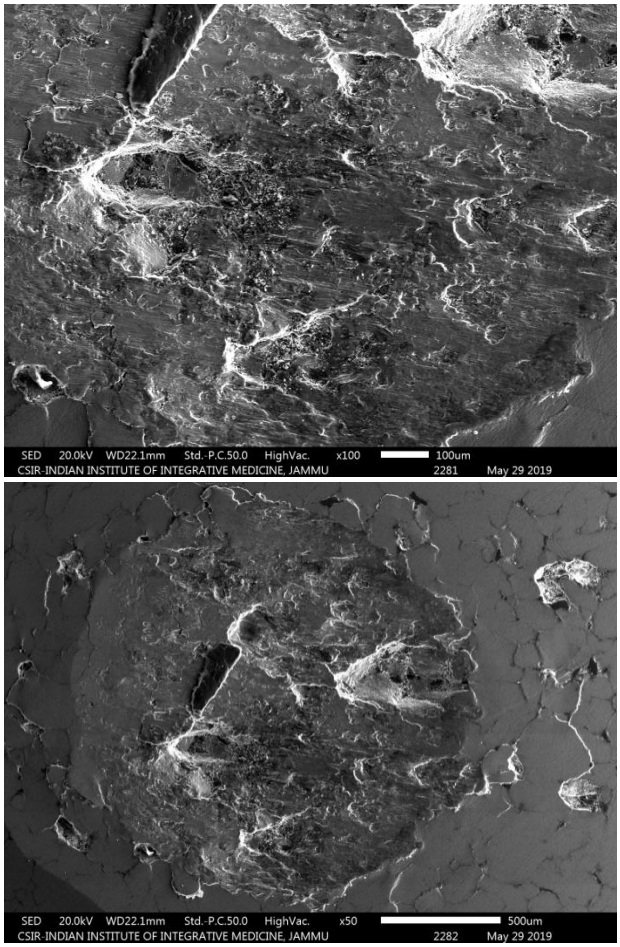

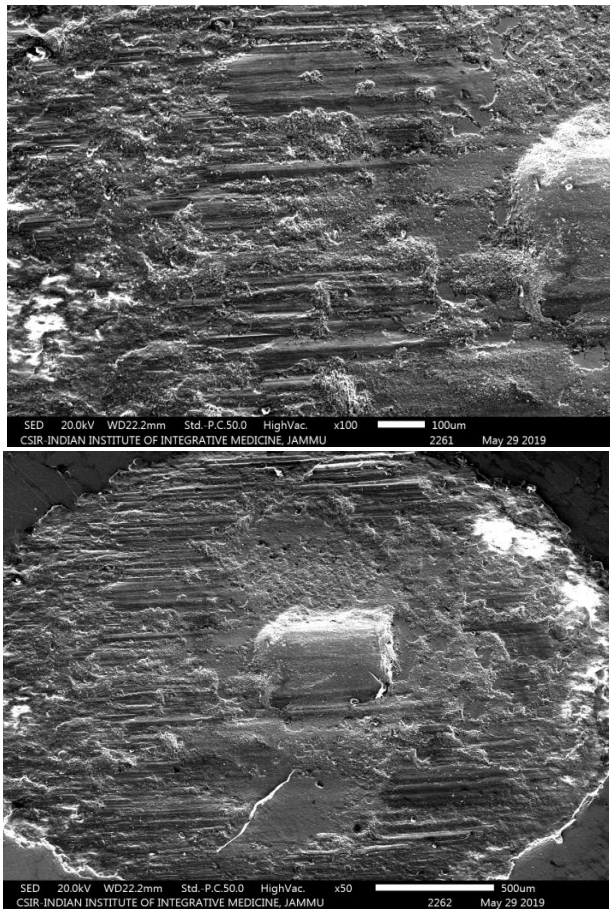

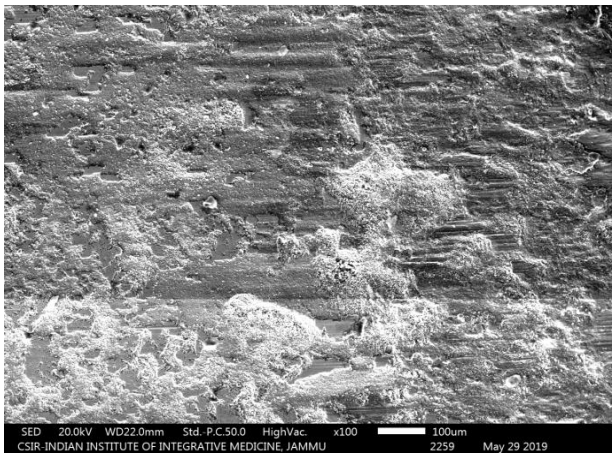

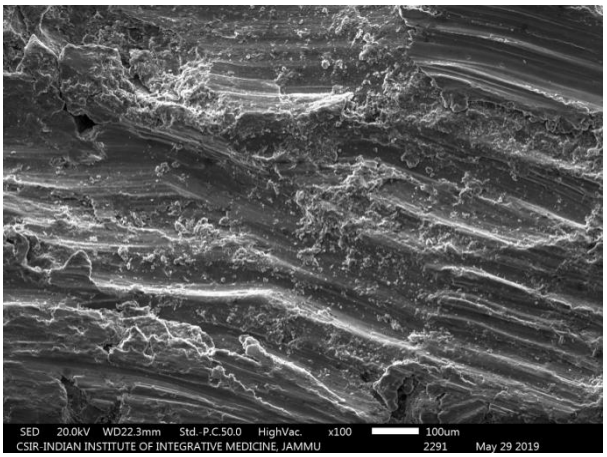

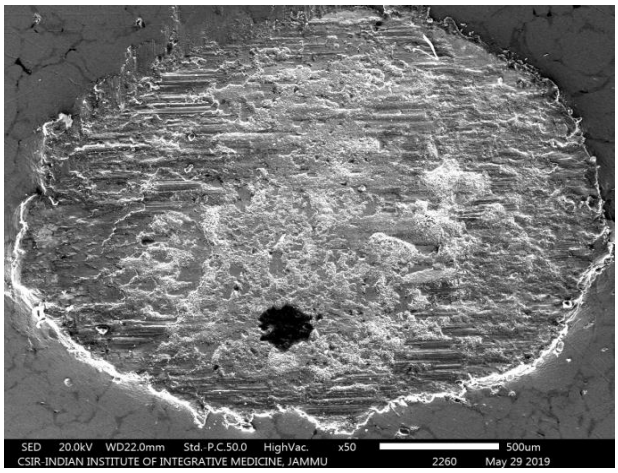

(b) Hybrid Composition 5 (500 ˚C)[50 N; 300 N; x50, x100]

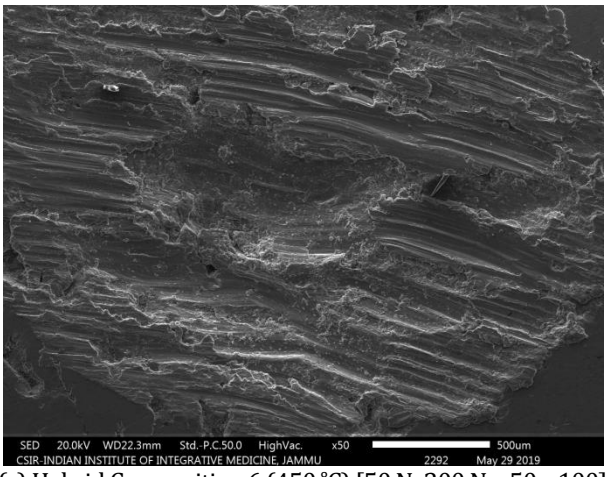

(c) Hybrid Composition 6 (450 ˚C) [50 N; 300 N; x50, x100]

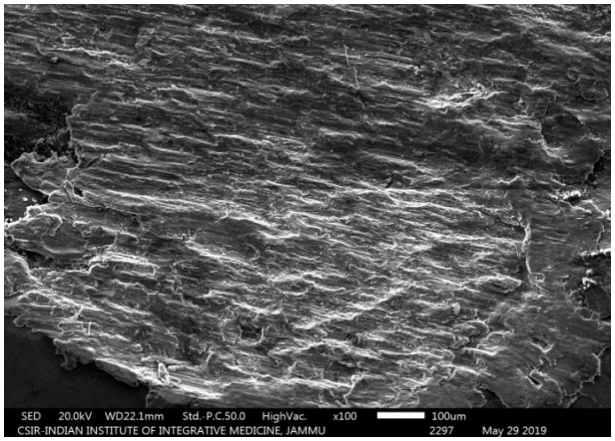

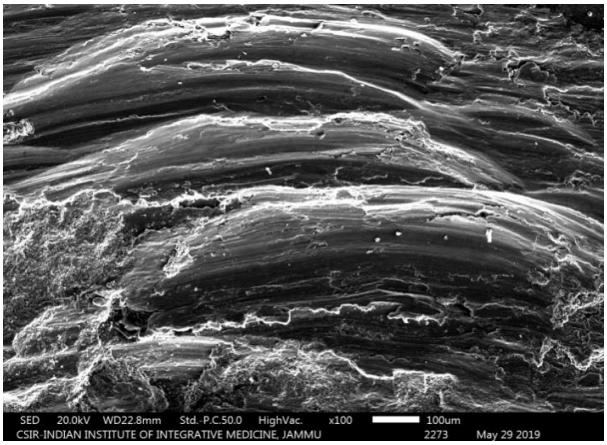

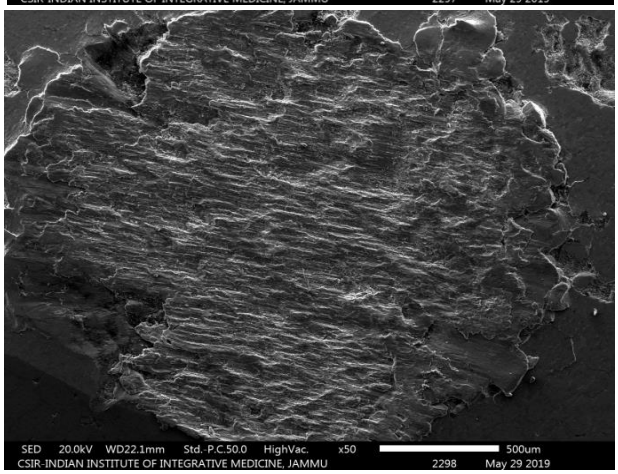

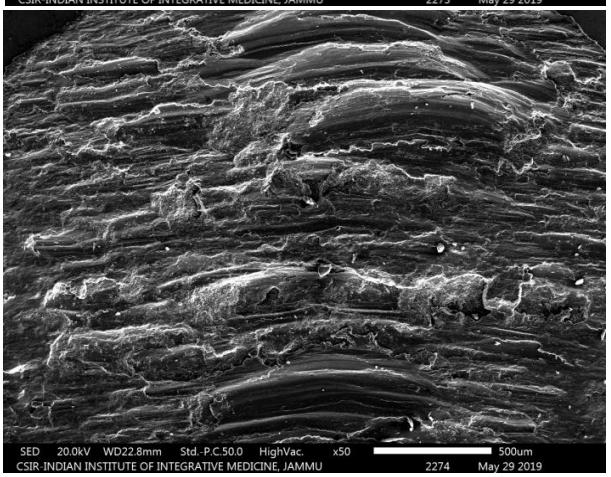

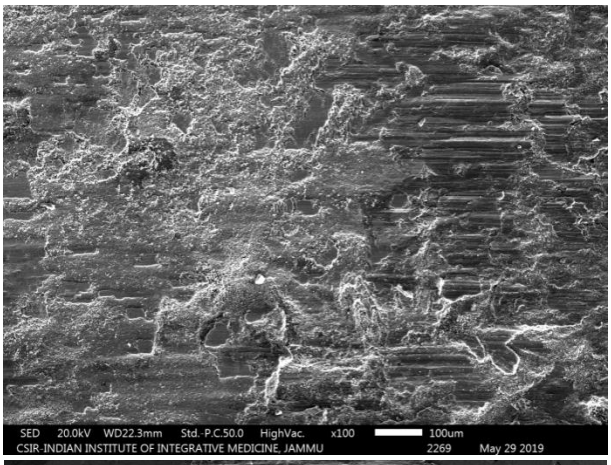

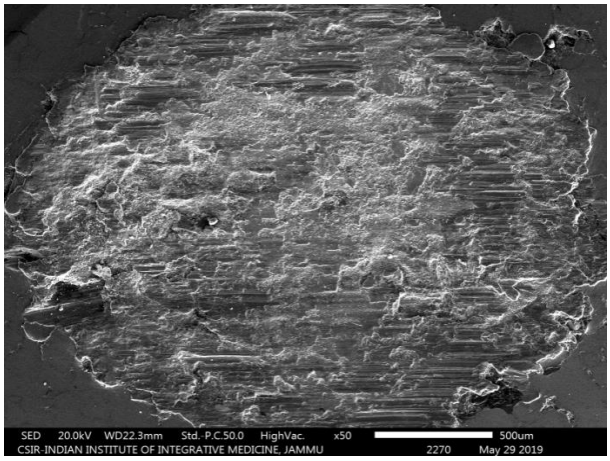

(d) Hybrid Composition 6 (500 ˚C) [50 N; 300 N; x50, x100]

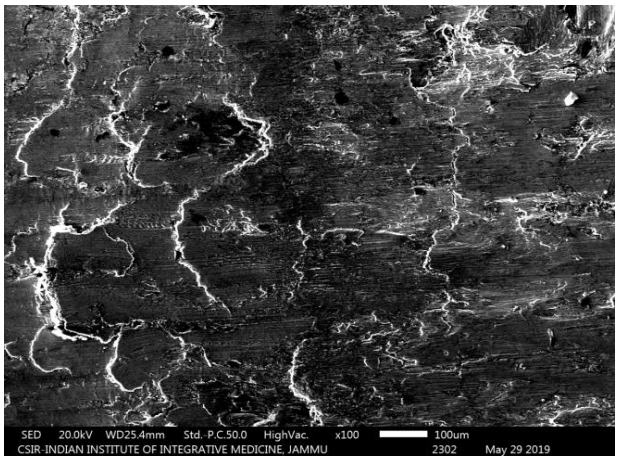

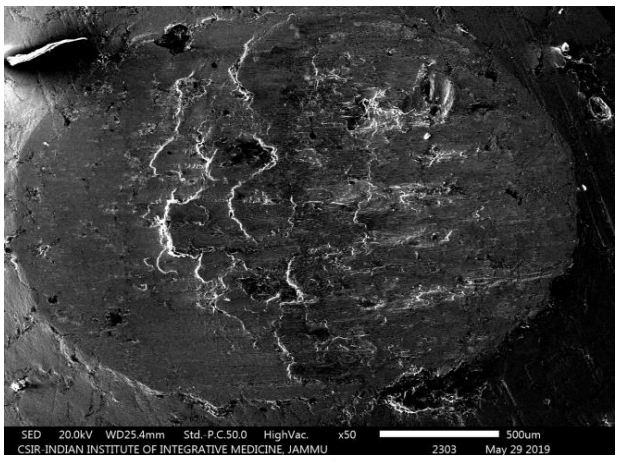

(e) Hybrid Composition 6 (520 ˚C) [50 N, 300 N; x50, x100]

Fig. 10. SEM Micrographs of the wear scar on hybrid composite sample and counter body.

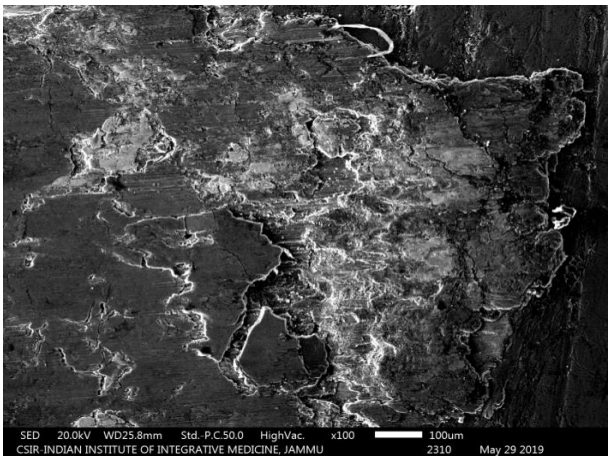

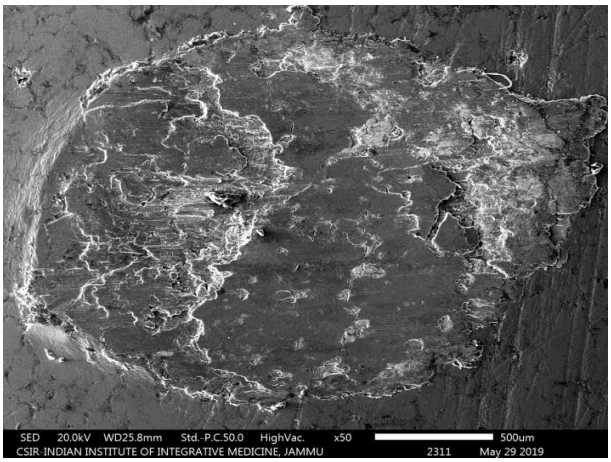

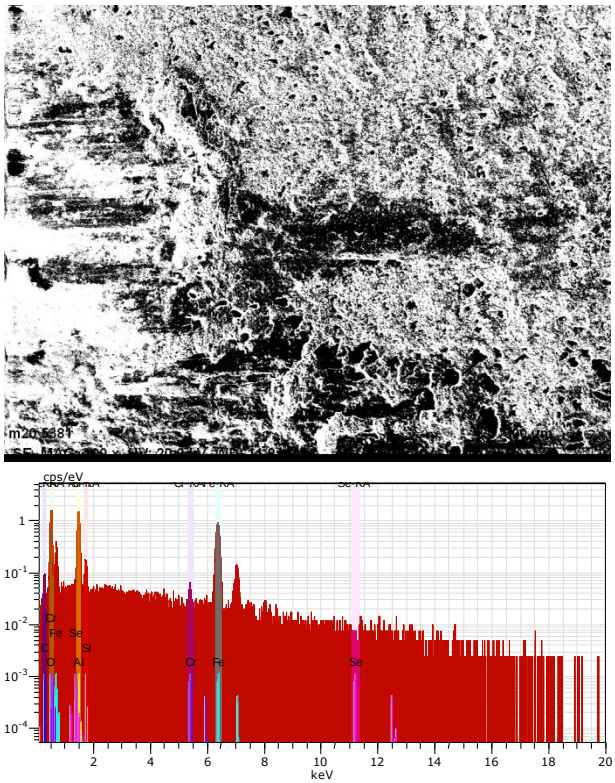

Fig. 11. EDS analysis of the wear scar.

Raman spectroscopy was carried on the GNP powder sample, as well as on the wear scar after tribo testing to evident the tribological behavior of the hybrid composite. Raman mapping of the wear scar shows that intense band D, G, and 2D at 1350 cm^{-1}, 1598 cm^{-1} and 2700 cm^{-1} peaks respectively (Fig. 12). These peaks conform the presence of graphene oxide layer which reduce friction and wear of hybrid composites. Results revels that deposited layer (smoother surface) reduces surface roughness, COF as well as wear of the material. Moreover, these protective layers fill the asperity-asperity gap of deep scratches and grooves and reduce wear of material.

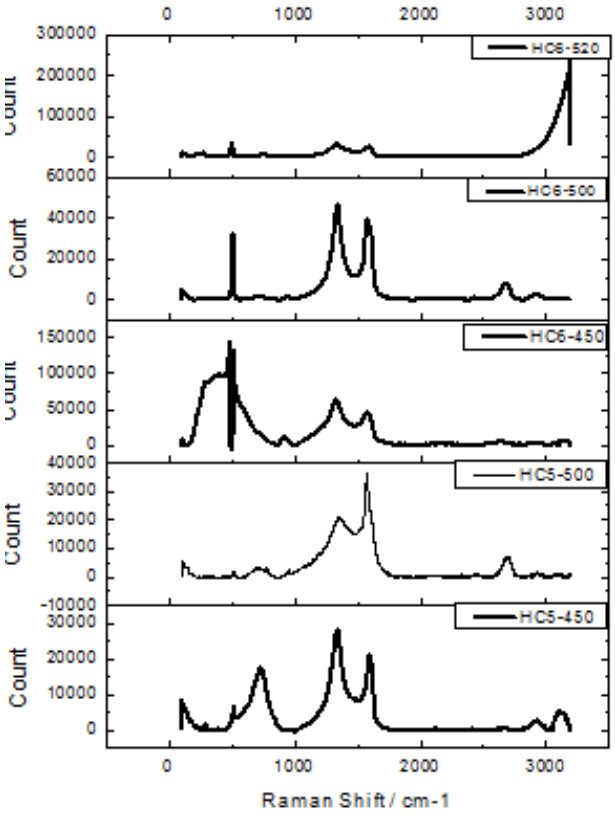

Fig. 12. Raman Shift of the wear scar.

For further analysis of the wear scar morphology; 3D Profilometer was used to analyze the scar roughness and texture (Fig. 13). In dry sliding test at high load for hybrid composite; HC5-450 shows the maximum surface roughness (Ra) of 3.4 µm at 50 N load. Further, increase in the load leads to reduced surface roughness and smooth layer, which is produced because of the presence of GNP, which act as the solid lubricant and forms a lubricating film at the scar interface. Surface roughness 2.9 µm, 2.5 µm and 2.2 µm were reported at 100 N, 200 N, 300 N load for HC5-450 respectively. HC6-520 shows minimum value for surface roughness of 0.9 µm at 300 N load.

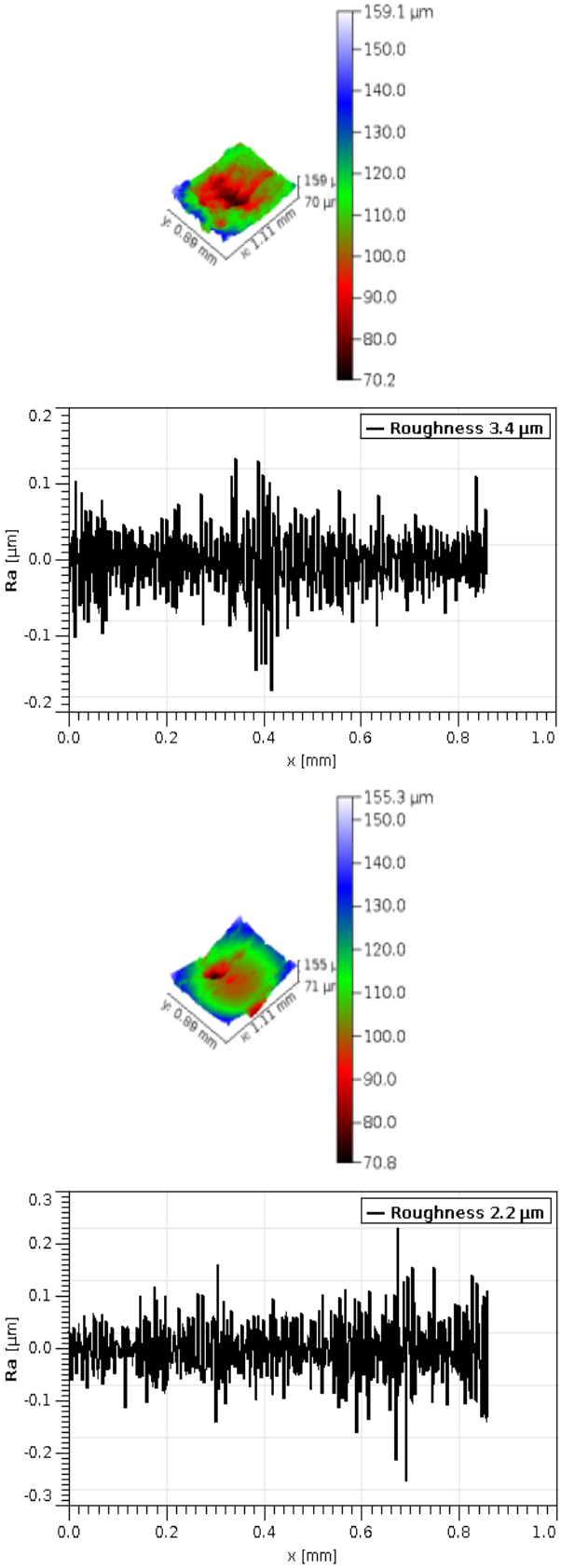

(a) Hybrid Composition 5 (450 °C) [50 N, 300 N]

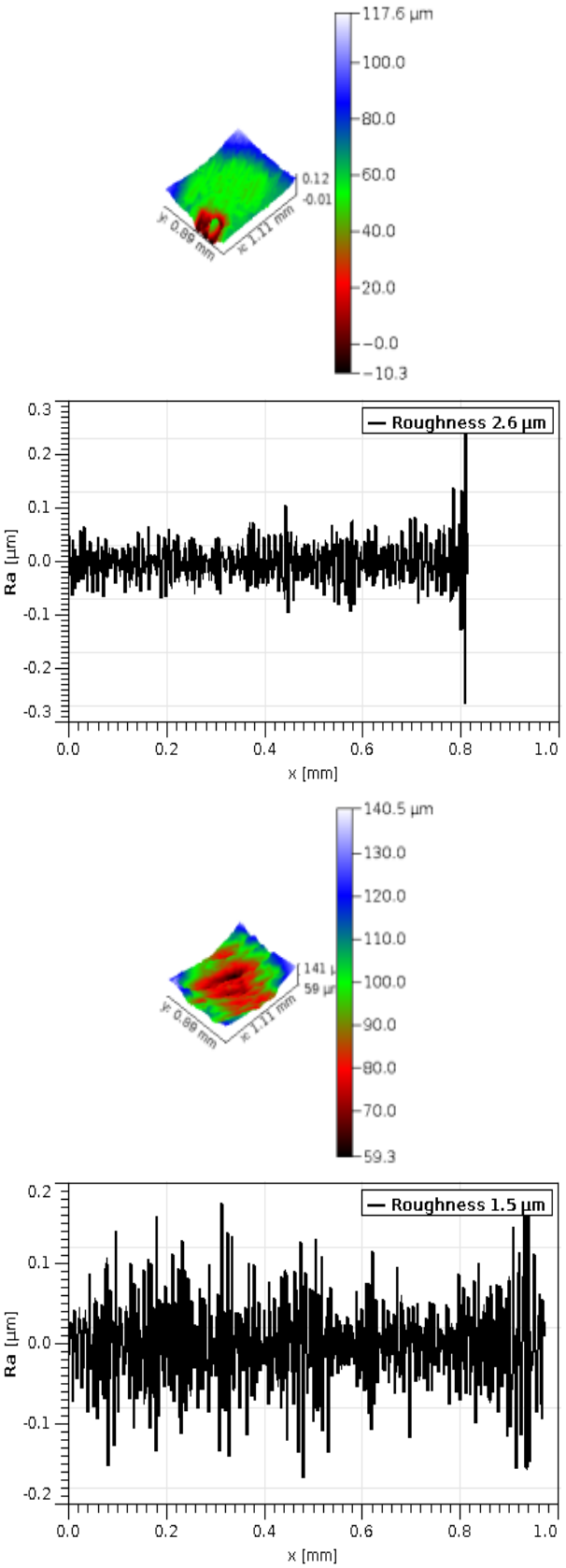

(b) Hybrid Composition 5 (500 °C) [50 N, 300 N]

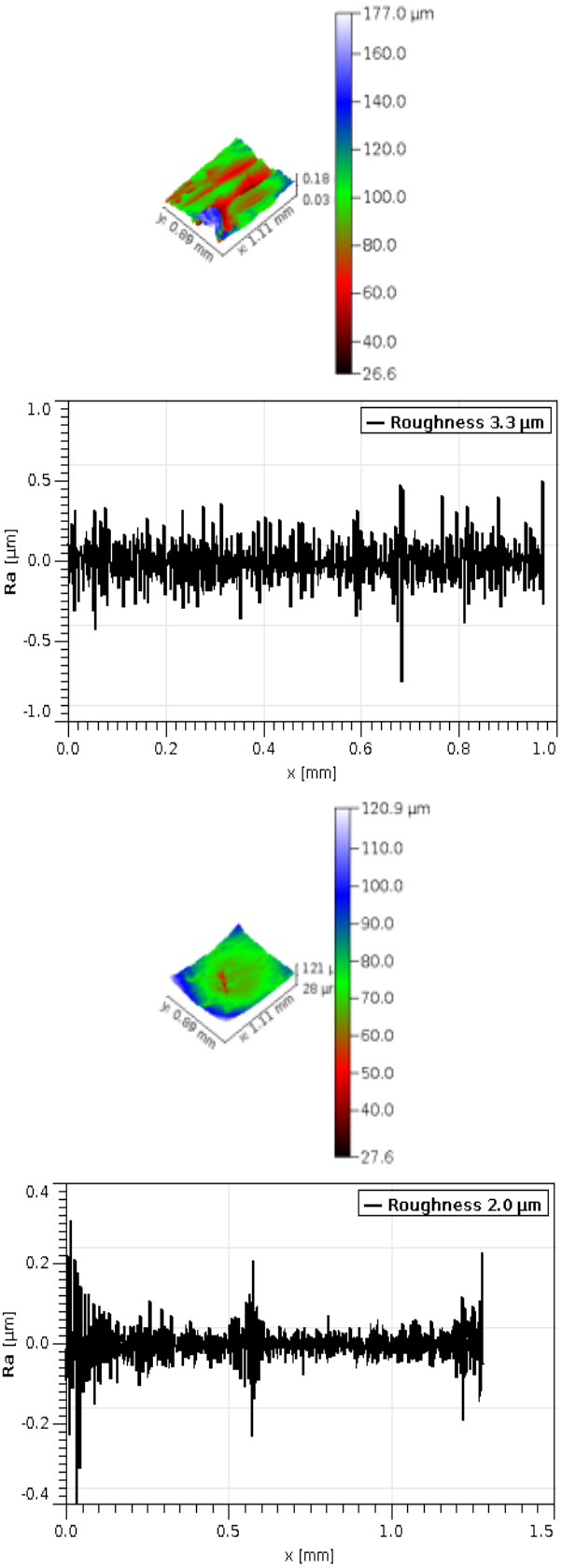

(c) Hybrid Composition 6 (450 °C) [50 N, 300 N]

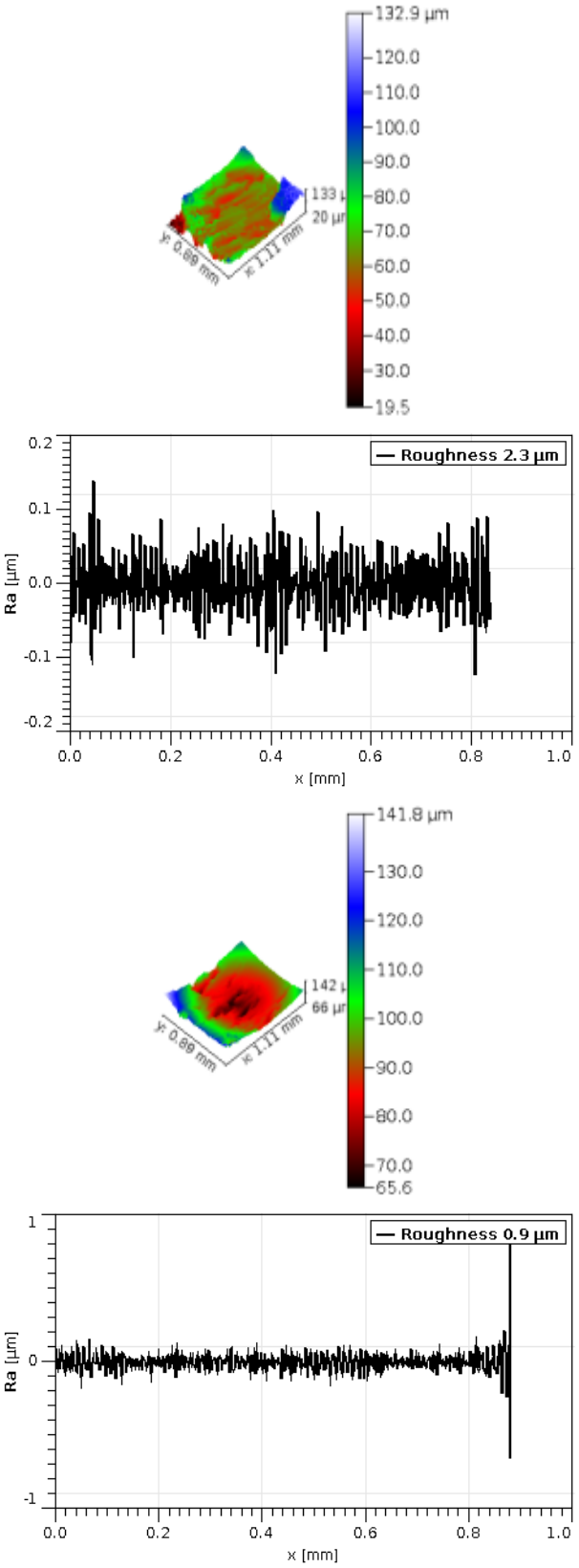

(e) Hybrid Composition 6 (520 °C) [50 N, 300 N]

Fig. 13. 3D-Profilometer analysis and surface roughness of the wear scar.

From the tribological testing and its analysis, it is reported that decrease in the friction coefficient with increasing GNP content as well as with increasing load is observed for these self-lubricating hybrid composite samples. This decrease in the coefficient friction with increasing load was attributed to high contact pressure severity over the asperities tips. This enormous contacting applied load, increases the interface temperature which indeed reduce yield strength; ultimately reduces wear rate of the hybrid composite sample. It is also observed that the reduction in the surface roughness also report with increasing GNP content and even at high loading conditions. This high contact load crushes and fracture the asperities make the surface to feel much smooth hence reduce the worn surface roughness. With the introduction of the GNP content the antifriction as well as anti wear properties of the composite sample increases. This increase in the properties of the composite sample is attributed to the weak layered lamellar structure of the GNP particles. These layered lamellar particles act as solid lubricant under tribo testing conditions. After the initial run-in-period these solid lubricant particles come between the sliding bodies and hence reduce metal-metal direct contact of mating surfaces. Further these GNP particles leads to tribo layer formation at the worn surface which enhances the friction and wear properties. As the sliding continuous the plastic deformed particles stick to the contacting surface further leads to formation of low stress – strain junction of lubrication film. This junction has good anti friction properties and shows wear protection behavior. This protecting lubrication film plays an important role in polishing the fractured surface causing easy sliding of the counter body hence reduce friction and wear.

6. CONCLUSION

1. In this present research, effect of high load, sintering temperature as well as the reinforcement concentration is studied. On the basis of result obtained it can be concluded that: that all three factors influence the tribological as well as mechanical properties of the hybrid composite samples. Spark Plasma Sintering fabrication route make it possible to achieve near thoritical dense sample. It is also observed that with an increase in the sintering temperature density increases and porosity of the composite sample decreases.

2. Introduction of the self-lubricating GNP reinforcement and hard phase alumina increases the tribological properties compared to matrix material.
3. Results of the tribo test indicate that the novel hybrid self lubricating composite exit excellent anti friction anf anti wear properties compared to Al-Si/nano Aluminium Oxide composite. Reduction in friction and wear of the hybrid composite was reported in the range 12.41 – 40 % and 87.76 – 92.97 % compared to Al-Si / Nano Aluminium Oxide composite sample.
4. The increase in the surface roughness due to sliding of the mating surface decreases by 50.22 – 79.63 % while using hybrid self lubricating composite sample compared to Al-Si/nano Aluminium oxide composite sample.
5. Also there is reduction in the surface roughness with increasing load for similar composition. This reduction ia attributed to high contact pressure at the asperities.
6. Adhesion, delamination, scuffing and melt wear are the dominant wear mechanisms. Formation of tribo-layer was also investigated in this study.

It was observed that addition of these reinforcements improves the overall properties of the nanocomposite materials.Significant results for the friction and wear were observed in the study. This study therefore, unlocks the significance of these materials for various tribological applications in automotive industry.

Acknowledgment

I gratefully acknowledge all the researchers who have worked in the field of tribology.Without their significant contribution, this review literature would have been difficult to summarise. I would also want to acknowledge my institute and supervisor for their wholehearted support.

REFERENCES

[1] K.G. Budinski, M.K. Budinski: *Engineering materials: Properties ans Selection, 9th Edition.* Pearson, 2010.

[2] N.P. Suh, *The delamination theory of wear*, Wear, vol. 25, iss. 1, pp. 111-124, 1973, doi: 10.1016/0043-1648(73)90125-7

[3] H.C. Meng, K.C. Ludema, *Wear models and predictive equations: their form and content*, Wear, vol. 181-183, pp. 443-457, 1995, doi: 10.1016/0043-1648(95)90158-2

[4] J.M. Challen, P.L.B. Oxley, *An explanation of the different regimes of friction and wear using asperity deformation models*, Wear, vol. 53, iss. 2, pp. 229-243, 1979, doi: 10.1016/0043-1648(79)90080-2

[5] B. Bhushan, J.N. Israelachvili, U. Landman, *Nanotribology: friction, wear and lubrication at the atomic scale*, Nature, vol. 374, pp. 607-616, 1995, doi: 10.1038/374607a0

[6] D.H. Buckley: *Surface effects in adhesion, friction, wear, and lubrication*. Elsevier, 1981.

[7] K.C. Ludema, L. Ajayi*: Friction, wear, lubrication: a textbook in tribology.* CRC press, 2018.

[8] L. Merhari, *Hybrid nanocomposites for nanotechnology*. Springer, 2009, doi: 10.1007/978-0-387-30428-1

[9] C. Sanchez, B. Julián, P. Belleville, M. Popall, *Applications of hybrid organic–inorganic nanocomposites*, Journal of Materials Chemistry, vol. 15, iss. 35-36, pp. 3559-3592, 2005, doi: 10.1039/B509097K

[10] G. Kickelbick: *Hybrid materials: synthesis, characterization, and applications*. John Wiley & Sons, 2007.

[11] M.L.T. Guo, C.-Y.A. Tsao, *Tribological behavior of self-lubricating aluminium/SiC/graphite hybrid composites synthesized by the semi-solid powder-densification method*, Composites Science and Technology, vol. 60, iss. 1, pp. 65-74, 2000, doi: 10.1016/S0266-3538(99)00106-2

[12] A.D. Moghadam, B.F. Schultz, J.B. Ferguson, E. Omrani, P.K. Rohatgi, N. Gupta, *Functional metal matrix composites: self-lubricating, self-healing, and nanocomposites-an outlook*, vol. 66, iss. 6, pp. 872-881, 2014, doi: 10.1007/s11837-014-0948-5

[13] M. Omori, *Sintering, consolidation, reaction and crystal growth by the spark plasma system (SPS),* Materials Science and Engineering: A, vol. 287, iss. 2, pp. 183-188, 2000, doi: 10.1016/S0921-5093(00)00773-5

[14] A.Z. Munir, U. Anselmi-Tamburini, M. Ohyanagi, *The effect of electric field and pressure on the synthesis and consolidation of materials: A review of the spark plasma sintering method*, Journal of Materials Science, vol. 41, iss. 3, pp. 763-777, 2006, doi: 10.1007/s10853-006-6555-2

[15] O. Guillon, J. Gonzalez-Julian, B. Dargatz, T. Kessel, G. Schierning, J. Räthel, M. Herrmann, *Field-assisted sintering technology/spark plasma sintering: mechanisms, materials, and technology developments,* Advanced Engineering Materials, vol. 16, iss. 7, pp. 830-849, 2014, doi: 10.1002/adem.201300409

[16] Y.B. Liu, J.D. Hu, Z.Y. Cao, P.K. Rohatgi, *Wear resistance of laser processed Al–Si–graphite composites*, Wear, vol. 206, iss. 1-2, pp. 83-86, 1997, doi: 10.1016/S0043-1648(96)07496-0

[17] C.B. Lin, R.J. Chang, W.P. Weng, *A study on process and tribological behavior of Al alloy/Gr.(p) composite*, Wear, vol. 217, iss. 2, pp. 167-174, 1998, doi: 10.1016/S0043-1648(98)00192-6

[18] L. Krishnamurthy, B.K. Sridhara, D.A. Budan, *Comparative study on the machinability aspects of aluminium silicon carbide and aluminium graphite composites*, Materials and Manufacturing Processes, vol. 22, no. 7-8, pp. 903-908, 2007, doi: 10.1080/10426910701451754

[19] S. Das, S.V. Prasad, T.R. Ramachandran, *Tribology of Al Si alloy-graphite composites: triboinduced graphite films and the role of silicon morphology*, Materials Science and Engineering: A, vol. 138, iss. 1, pp. 123-132, 1991, doi: 10.1016/0921-5093(91)90682-D

[20] M.L.T. Guo, C.-Y.A. Tsao, *Tribological behavior of self-lubricating aluminium/SiC/graphite hybrid composites synthesized by the semi-solid powder-densification method*, Composites Science and Technology, vol. 60, no. 1, pp. 65-74, 2000, doi: 10.1016/S0266-3538(99)00106-2

[21] M.L.T. Guo, C.-Y.A. Tsao, *Tribological behavior of aluminum/SiC/nickel-coated graphite hybrid composites,* Materials Science and Engineering: A, vol. 333, iss. 1-2, pp. 134-145, 2002, doi: 10.1016/S0921-5093(01)01817-2

[22] A.M. Hassan, A.S. Al-Bsharat, *Influence of burnishing process on surface roughness, hardness, and microstructure of some non-ferrous metals*, Wear, vol. 199, no. 1, pp. 1-8, 1996, doi: 10.1016/0043-1648(95)06847-3

[23] A.R. Riahi, A.T. Alpas, *The role of tribo-layers on the sliding wear behavior of graphitic aluminum matrix composites*, Wear, vol. 251, iss. 1-12, pp. 1396-1407, 2001, doi: 10.1016/S0043-1648(01)00796-7

[24] S. Basavarajappa, G. Chandramohan, K. Mukund, M. Ashwin, M. Prabu, *Dry sliding wear behavior of Al 2219/SiCp-Gr hybrid metal matrix composites*, Journal of Materials Engineering and Performance, vol. 15, iss. 6, p. 668, 2006, doi: 10.1361/105994906X150803

[25] P.K. Rohatgi, R. Guo, J.K. Kim, S. Rao, T. Stephenson, T. Waner, *Wear and friction of cast Al–SiC–Gr composites*, in: Proceedings of materials solutions '97 on wear of engineering materials, 15–18 September, 1997, Indianapolis, Indiana, pp. 205-211.

[26] A. Ghazaly, B. Seif, H.G. Salem, *Mechanical and tribological properties of AA2124-grapheneself-lubricating nanocomposite*, Light Metals 2013, pp. 411-415, 2016, doi: 10.1007/978-3-319-65136-1_71

[27] F.P. Bowden, D. Tabor, *The area of contact between stationary and moving surfaces*, Proceedings of the Royal Society of London. Series A, Mathematical and Physical Sciences, vol. 169, iss. 938, pp. 391-413, 1939, doi: 10.1098/rspa.1939.0005

[28] G.J. Howell, A. Ball, *Dry sliding wear of particulate-reinforced aluminium alloys against automobile friction materials*, Wear, vol. 181-183, pp. 379-390, 1995, doi: 10.1016/0043-1648(95)90045-4